Journal of Engineering Mathematics, Vol. 3, No. 1, January 1969
Wolters-Noordhoff Publishing – Groningen
Printed in the Netherlands

On the Optimum One-Bladed Cycloidal Ship Propeller

J. A. SPARENBERG AND R. DE GRAAF

Dept. of Mathematics, University of Groningen, Groningen, the Netherlands

(Received August 7, 1968)

SUMMARY

The optimal motion of a one-bladed cycloidal propeller is investigated by minimizing the kinetic energy, left behind in the wake. The propeller blade is assumed to perform a, fish tail like, trochoidal motion and to provide a prescribed thrust. The theory is two-dimensional. The efficiency of the propeller is calculated and its quality is discussed.

1. Introduction

The propeller, we will discuss here, can be considered to belong to the class of the cycloidal propellers [5]. We first give a schematic description of its special properties.

The propeller possesses an axis of rotation, perpendicular to the bottom of the ship (Fig. 1.1). At the lower end of this axis and parallel to the bottom we can imagine a circular disc, to which the propeller blades are attached. These blades are perpendicular to the disc and during the rotation of the disc they perform an oscillatory motion around short shafts. The points, where these shafts meet the disc, are denoted by T'. The angular velocity ω of the disc is constant.

We will determine the oscillatory motion of the blades in such a way that, under a certain constraint which will be discussed later on, the efficiency of the propeller is as high as possible.

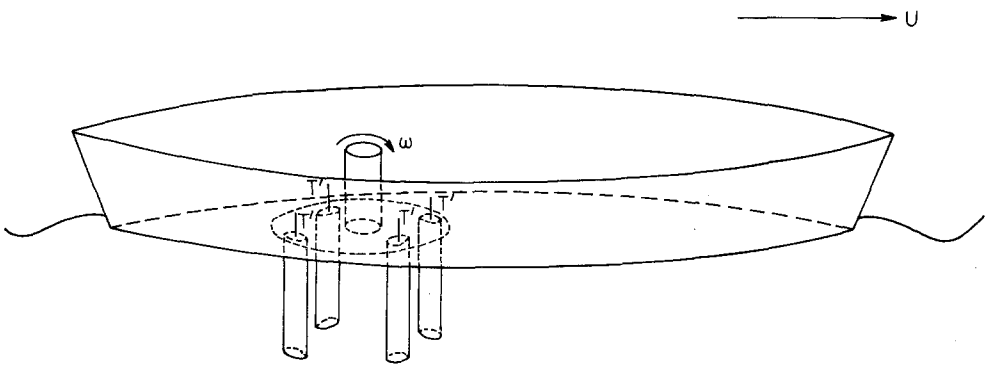

Figure 1.1. Scheme of a ship with a cycloidal propeller.

In the ordinary case the rotational velocity ωR of the propeller blades, where R denotes the distance from the turning points T' to the axis of the propeller, is large with respect to the translation velocity U of the ship. Fig. 1.2 shows the self-intersecting orbits of the blades in a cross section, parallel to the surface of the fluid. Here we consider, however, the case, that the rotational velocity is sufficiently small. Then the blades move like a fish tail (Fig. 1.3).

Besides this we assume, that the propeller is provided with only one blade (Fig. 1.3). We notice, that the presence of more blades will of course influence the optimal oscillatory motion of the blades. Hence more complicated calculations will be needed in the future.

The propeller is placed in water, here considered as an incompressible and inviscid fluid. We assume, the blade is infinitely long. Hence we ignore tip effects. Besides we suppose, the

blade is infinitely thin and has no twist, while the chord length at every height will be the same. Therefore we have a two-dimensional problem. Further the chord length will be small with respect to the smallest radius of curvature of the orbit of the blade. This restriction, as is discussed in [6] and [7], is essential for the linear theory, we will describe here. As contrasted

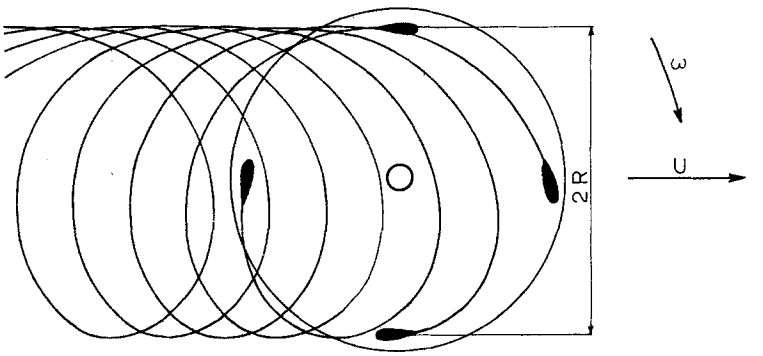

Figure 1.2. Self-intersecting orbits.

with [6] we take into account the real chord length. This will be done in a manner, consistent with the linear theory.

Because the bound vorticity of the blade is varying, free vorticity and hence kinetic energy is left behind (Fig. 1.3). We will minimize this kinetic energy. In this way we obtain a variational problem for a vorticity function, which is connected with the free vorticity distribution in the wake, under the constraint, that the mean thrust per unit of length of the blade with respect to time has a prescribed value. Besides this we will apply another method, given in [7], to obtain the above-mentioned vorticity function, belonging to the optimal motion of the propeller. With this method the vorticity function can be calculated numerically from a mixed boundary-value problem or be measured with the aid of an electrolytic tank.

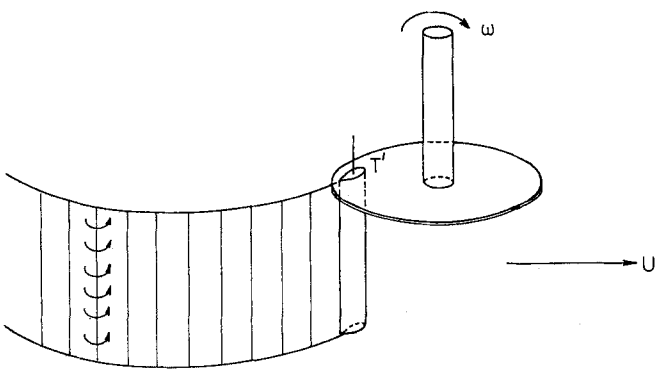

Figure 1.3. The one-bladed propeller with the free vortex layer.

From the vorticity function follows easily the efficiency of the optimum propeller. It will be shown that the propeller has a rather small quality coefficient. This coefficient is defined in section 10. It follows that it is most likely that fish propulsion is not nearly so beautiful as generally is thought.

Also we determine the angle of incidence of the blade as a function of time for the optimum propeller. Results for this angle of incidence will be compared with results, following from the theory of [6], by which we can obtain insight in the influence of the finite chord length.

For a detailed discussion of several derivations and the numerical calculations which are to a certain extent suppressed in this article, we refer to [9].

2. Bound and Free Vorticity

As assumed in the introduction we have a two-dimensional problem. Hence, we consider in the following a profile A′B′ of chord length l, moving in a flat plane. In this plane we choose a Cartesian coordinate system (x, y), which is at rest with respect to the fluid (Fig. 2.1).

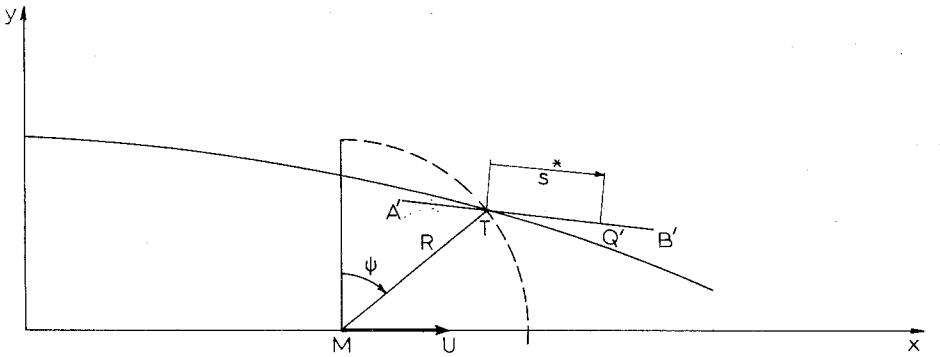

Figure 2.1. The profile A′B′ in the (x, y)-plane.

As a reference point at the profile we take the perpendicular projection T of the turning point T' on the (x, y)-plane (Figs. 1.3 and 2.1). The distance from T to a point Q' at the profile A′B′ is denoted by s^*. This distance is measured positive in the direction of the leading edge of the profile. In the following T will be chosen outside of the profile (Fig. 2.2), which is not essential. The point T rotates with a constant angular velocity ω around the point M at the x-axis, while M moves with a constant velocity U in the positive x-direction.

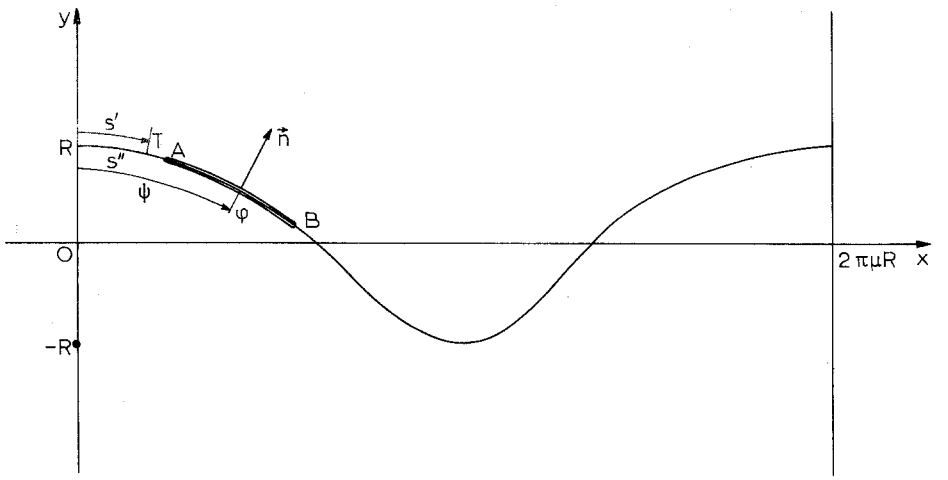

Figure 2.2 The cycloidal orbit of T with the segment AB.

The orbit of T then becomes a cycloid (Fig. 2.2):

$$x = R(\mu\psi + \sin\psi),\quad y = R\cos\psi\,;\quad \mu = U/\omega R\,, \tag{2.1}$$

$$\psi = \omega t\,, \tag{2.2}$$

where R is the radius MT of the circle, ψ the angular coordinate of T and t the time. We assume in the following $\mu > 1$. Then the cycloid does not intersect itself. Such a cycloid is called a trochoid. In that case the motion of the blade resembles, to a certain extent, the motion of the tail of a fish.

For the theoretical investigation we make use of a linearization process. We replace the

profile A′B′ by a segment AB of the cycloid, on which we have a time dependent bound vorticity (Fig. 2.2). This segment has a fixed length l and moves along the cycloid with a velocity, of which the magnitude in every point of it equals the magnitude of the velocity of T. The segment has to deform itself during the motion because of the varying curvature of the cycloid.

We will understand by a point at the cycloid a point, fixed with respect to the cycloid. By a point of AB we understand a point, fixed with respect to the segment AB. Hence such a point will move along the cycloid. Now a point Q of AB possesses two coordinates, viz. φ and s (Fig. 2.3). The coordinate φ is the angular coordinate of the point at the cycloid, which just at that moment coincides with Q, and s is the distance from T to Q along the cycloid. This distance is positive, if Q lies in the translation direction of the segment AB. The distances from T to the trailing edge and to the leading edge of the segment AB are denoted by respectively a and $a+l$. If a is negative, T is at AB.

The points of the actual profile A′B′ are mapped on the points of AB in such a way, that $s=s^*$. We suppose, the chord length l to be small with respect to the smallest radius of curvature of the cycloid.

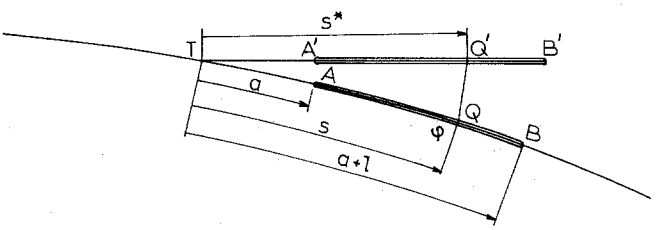

Figure 2.3. The position of the segment AB.

The magnitude of the velocity of a point of AB, which, as has been said, equals the magnitude of the velocity of T, is denoted by $V(\psi)$. According to (2.1) there holds, s' being the distance from a fixed point at the cycloid to T, measured along the cycloid (Fig. 2.2):

$$\frac{ds'}{d\psi} = \left\{\left(\frac{dx}{d\psi}\right)^2 + \left(\frac{dy}{d\psi}\right)^2\right\}^{\frac{1}{2}} = R(1+\mu^2+2\mu\cos\psi)^{\frac{1}{2}} \overset{\text{def.}}{=} Rf(\psi). \tag{2.3}$$

From (2.2) and (2.3) we find for the velocity $V(\psi)$:

$$V(\psi) = \frac{ds'}{dt} = \frac{ds'}{d\psi}\omega = \omega R f(\psi). \tag{2.4}$$

The bound vorticity per unit of length in chordwise direction, at a point of AB with coordinates φ and s, is represented by $\Gamma(\varphi, s)$. This vorticity is given a positive value, if the corresponding flow is counterclockwise. We write for the derivative of $\Gamma(\varphi, s)$ with respect to φ:

$$\frac{\partial\Gamma(\varphi, s)}{\partial\varphi} = \dot{\Gamma}(\varphi, s).$$

Consider a point φ at the cycloid, where an element of length ds of AB, with the bound vorticity $\Gamma(\varphi, s)ds$, passes. If s remains constant and φ varies with $\Delta\varphi$, this bound vorticity will vary with $\dot{\Gamma}(\varphi, s)ds\Delta\varphi$. Denoting by s'' the distance, from a fixed point at the cycloid to the point φ, measured along the cycloid (Fig. 2.2), there holds according to (2.3):

$$\Delta\varphi = \frac{\Delta s''}{Rf(\varphi)}.$$

Hence it is obvious, that in the point φ free vorticity is left behind, of which the strength per unit of length amounts to

$$-\frac{\dot{\Gamma}(\varphi, s)ds}{Rf(\varphi)}. \tag{2.5}$$

If we want to have the total free vorticity $\gamma(\varphi, s)$ in the point (φ, s) of AB, we have to integrate over all free vorticity, which is shed at the point φ at the cycloid by the first part of AB. Using (2.5) we find:

$$\gamma(\varphi, s) = -\int_s^{a+l} \frac{\dot{\Gamma}(\varphi, \tau)}{Rf(\varphi)} d\tau = -\frac{1}{Rf(\varphi)} \int_s^{a+l} \dot{\Gamma}(\varphi, \tau) d\tau . \tag{2.6}$$

When the whole segment AB has passed the point φ at the cycloid, the free vorticity remains constant at that point. This vorticity has the value

$$\gamma(\varphi) \overset{\text{def.}}{=} \gamma(\varphi, a) = -\frac{1}{Rf(\varphi)} \int_a^{a+l} \dot{\Gamma}(\varphi, \tau) d\tau . \tag{2.7}$$

For the further calculations it is desirable to introduce here a vorticity function $g(\varphi)$, defined as follows:

$$g(\varphi) \overset{\text{def.}}{=} \int_a^{a+l} \Gamma(\varphi, s) ds . \tag{2.8}$$

This function $g(\varphi)$ represents the integral over all bound vorticity, which passes the point φ at the cycloid. According to (2.7) and (2.8) we have the following relation between this vorticity function $g(\varphi)$ and the free vorticity $\gamma(\varphi)$:

$$\gamma(\varphi) = -\frac{\dot{g}(\varphi)}{Rf(\varphi)}, \tag{2.9}$$

where

$$\dot{g}(\varphi) = \frac{dg(\varphi)}{d\varphi} .$$

3. The Thrust

In order to calculate the thrust we need the unit normal in the point φ at the cycloid. The tangent of the angle, between this vector $\boldsymbol{n}$ (Fig. 2.2) and the positive x-direction, equals $-dx/dy$. Therefore we find according to (2.1):

$$\boldsymbol{n} = \frac{(\sin \varphi, \mu + \cos \varphi)}{f(\varphi)} . \tag{3.1}$$

As assumed in the foregoing, the velocity of the axis of the propeller has a constant value U in the x-direction. Hence, if $K_x(t)$ denotes the x-component of the force, acting on the bound vorticity of AB, at the moment t, there holds for the useful work E_u per period, delivered by this force, according to (2.2):

$$E_u = U \int_0^{2\pi/\omega} K_x(t) dt .$$

Therefore, in order to minimize the kinetic energy, left behind in the wake, we will prescribe the mean value $K_x = \omega E_u / 2\pi U$ of the thrust $K_x(t)$. This prescribed value K_x yields a constraint on $g(\varphi)$. For finding this constraint we introduce a new function for the bound vorticity of AB:

$$G(\psi, s) \overset{\text{def.}}{=} \Gamma(\varphi, s) , \tag{3.2}$$

where ψ is the angular coordinate of T. Using (2.3) it is easy to find the following relation between φ and ψ:

$$s = R \int_\psi^\varphi f(\chi)\ d\chi . \tag{3.3}$$

If s is constant, it follows from (3.3):

$$\frac{d\psi}{d\varphi} = \frac{f(\varphi)}{f(\psi)} \quad (s \text{ is constant}). \tag{3.4}$$

By virtue of the law of Kutta–Joukowski the lift force

$$\rho V(\psi)\, G(\psi, s) ds$$

acts on an elementary bound vortex $G(\psi, s)ds$, which moves with the velocity $V(\psi)$, when ρ denotes the density of the fluid.

This force has the direction of the normal $\boldsymbol{n}$ at the point φ of the cycloid. According to (3.1) we find for the component in the x-direction:

$$\rho V(\psi)\, G(\psi, s) ds \frac{\sin\varphi}{f(\varphi)}.$$

Substitution of (2.4) and integration yields:

$$K_x = \frac{\rho\omega R}{2\pi} \int_a^{a+l} \left\{ \int_0^{2\pi} G(\psi, s) \sin\varphi \frac{f(\psi)}{f(\varphi)} d\psi \right\} ds, \tag{3.5}$$

where $\varphi = \varphi(\psi, s)$ according to (3.3). Making use of (3.2) and (3.4) we can rewrite (3.5):

$$K_x = \frac{\rho\omega R}{2\pi} \int_a^{a+l} \left\{ \int_{\varphi^*}^{\varphi^*+2\pi} \Gamma(\varphi, s) \sin\varphi\, d\varphi \right\} ds,$$

where by virtue of (3.3) φ^* depends on s in the following way:

$$s = R \int_0^{\varphi^*} f(\chi) d\chi.$$

Because of the periodicity of the integrand is

$$\int_{\varphi^*}^{\varphi^*+2\pi} \Gamma(\varphi, s) \sin\varphi\, d\varphi = \int_0^{2\pi} \Gamma(\varphi, s) \sin\varphi\, d\varphi.$$

Therefore, using (2.8), we find:

$$K_x = \frac{\rho\omega R}{2\pi} \int_0^{2\pi} g(\varphi) \sin\varphi\, d\varphi. \tag{3.6}$$

The mean value K_y of the y-component of the force is obtained analogously:

$$K_y = \frac{\rho\omega R}{2\pi} \int_0^{2\pi} g(\varphi)(\mu + \cos\varphi) d\varphi. \tag{3.7}$$

In connection with an additional condition, which can be imposed on $g(\varphi)$, it turns out in section 6, that K_y becomes zero automatically.

We remark that we neglect the suction force at the leading edge, because the angles between the normals $\boldsymbol{n}$ at the cycloid and the x-direction are finite, nearly everywhere. Hence in a linear theory this second order force can be neglected.

4. The Velocity Potential

For the evaluation of the kinetic energy we need the velocity potential difference across the cycloid in a point φ_0 at the cycloid, when the segment AB has already passed. We denote the potential with Φ. By the $\pm$ side of the cycloid we will understand that side, which can be reached from the region $y \gtrless R\cos\varphi$ (Figs. 4.1 and 2.2).

In order to determine the potential difference we consider the segment AB, when the trailing edge A is at φ_0. It is found easily that

$$\Phi_+(\varphi_0) - \Phi_-(\varphi_0) = \int_{AB} \{\boldsymbol{v}_-(s) - \boldsymbol{v}_+(s)\} \cdot d\boldsymbol{s} \overset{\text{def.}}{=} \int_a^{a+l} G_{\text{tot}}(\psi_0, s) ds, \tag{4.1}$$

where $\boldsymbol{v}_+(s)$ is the velocity vector of the fluid at the + side of the cycloid and $\boldsymbol{v}_-(s)$ the velocity vector of the fluid at the − side of the cycloid, while ds denotes an infinitesimal distance vector, which is tangent to the cycloid. Further ψ_0 is the angular coordinate of T at that moment, so that $\psi_0 = \psi_0(\varphi_0, a)$ according to (3.3).

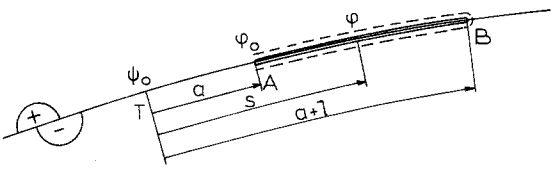

Figure 4.1. Determination of the potential difference across the cycloid.

We can simplify the last integral in (4.1) by remarking, that $g(\varphi_0)$, although defined by (2.8), satisfies the relation

$$g(\varphi_0) = \int_a^{a+l} \{\Gamma(\varphi, s) + \gamma(\varphi, s)\}\, ds\,, \tag{4.2}$$

where $\varphi = \varphi(s)$ follows from (3.3) when we take there $\psi = \psi_0$.

This can be proved by using the following simple property of the vorticity. After having passed the point φ_0 at the cycloid, an elementary bound vortex of AB gives rise to the creation of free vorticity. The sum of this created free vorticity and the variation of the bound vorticity remains every moment zero. This statement is in essence formula (4.2). An analytical proof of (4.2) is given in [9].

From (4.1) and (4.2), we see that

$$\Phi_+(\varphi_0) - \Phi_-(\varphi_0) = g(\varphi_0)\,. \tag{4.3}$$

If the segment AB has passed the point φ_0, the potential difference in that point remains constant. For at every moment the variation of the bound vorticity is compensated by the creation of free vorticity. Analytically this is proved in [9].

Next we want to know the potential difference over a period far behind the segment AB. We assume, that the segment AB is at $x = +\infty$. According to [6], formula (3.5), there holds:

$$\Phi(x + 2\pi\mu R, y) - \Phi(x, y) = 0\,, \quad |y| > R\,.$$

From this we find immediately the potential difference over a period for $|y| \leqq R$.

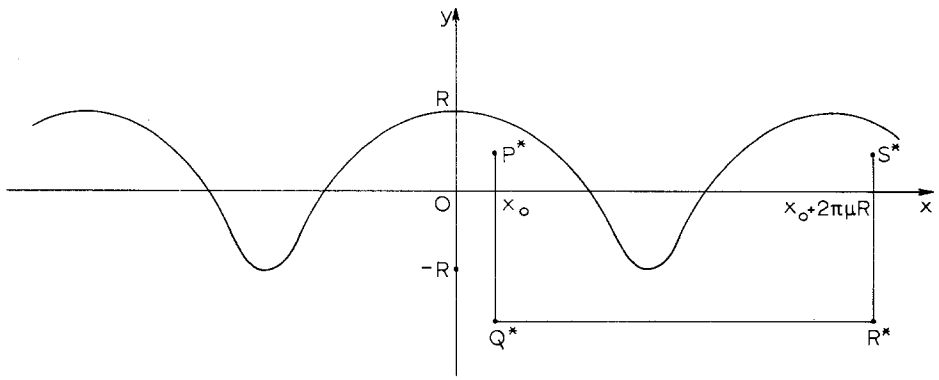

Figure 4.2. Determination of the potential difference over a period.

Considering the potential along $P^*Q^*R^*S^*$ (Fig. 4.2), it is clear, that by reasons of periodicity the potential differences over P^*Q^* and S^*R^* are equal. Hence there holds for each y, with exception of the points, lying at the cycloid, where the potential is not defined:

$$\Phi(x+2\pi\mu R, y)-\Phi(x, y)=0\,. \tag{4.4}$$

We remark, that formula (3.7) of [6] for the potential difference, in case of $|y|<R$, is wrong and has to be replaced by (4.4). The mistake in [6] is caused by the fact, that in calculating the potential difference "implicitly" the vortex layer has been traversed.

5. The Kinetic Energy

When the thrust is prescribed, the kinetic energy, left behind per period, has to be as small as possible for an optimum propeller. Assuming the segment AB at $x=+\infty$, we calculate the

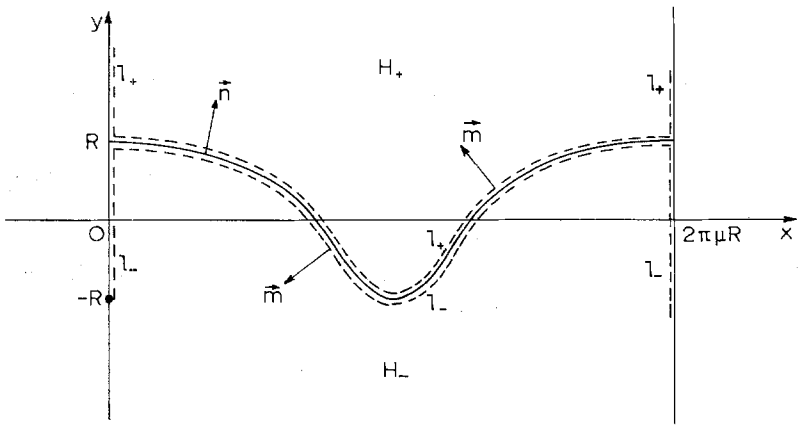

Figure 5.1. Determination of the kinetic energy per period.

kinetic energy E of the fluid over one period far behind the segment, viz. in a vertical strip H (Fig. 5.1) with

$$0\leqq x\leqq 2\pi\mu R\,,$$
$$-\infty\leqq y\leqq+\infty\,.$$

This is done in the same way as in [6]. We divide H into two subregions, viz. H_+ and H_-, respectively above and beneath the cycloid. Both in H_+ and in H_- we have a velocity potential $\Phi(x, y)$. This potential has a jump at the cycloid, as follows from section 4. We have the following line integral for the energy E:

$$E=\tfrac{1}{2}\rho\iint_{H_++H_-}\left\{\left(\frac{\partial\Phi}{\partial x}\right)^2+\left(\frac{\partial\Phi}{\partial y}\right)^2\right\}dx\,dy=-\tfrac{1}{2}\rho\int_{l_++l_-}\Phi\frac{\partial\Phi}{\partial m}\,dl_+, \tag{5.1}$$

where l_+ and l_- represent the boundaries of respectively H_+ and H_- and $\partial\Phi/\partial m$ is the derivative of Φ in the direction of the inward unit normal $\boldsymbol{m}$ of l_+ or l_-.

According to [6], formula (3.3), there holds for the potential $\Phi(x, y)$ in an arbitrary point of the fluid, far behind the segment AB:

$$\Phi(x, y)=\mathrm{Re}\,\frac{R}{2\pi i}\int_0^{2\pi}\gamma(\theta)\log\left\{\sin\left(\frac{z-\zeta}{2\mu R}\right)\right\}f(\theta)d\theta+c_0\,, \tag{5.2}$$

where Re means "the real part of" and c_0 denotes a constant. Further $z=x+iy$ is a point in the complex (x, y)-plane and ζ a variable point at the cycloid in the complex plane:

$$\zeta=\xi+i\eta=R(\mu\theta+\sin\theta+i\cos\theta)\,. \tag{5.3}$$

By a limit consideration we find, that $\Phi(x, y)$ at $y=\pm\infty$ becomes constant. Hence the parts of $l_\pm$ at $y=\pm\infty$ yield no contribution to the line integral E. Further it is easy to show, that the contributions from the vertical parts of $l_\pm$ to the line integral cancel each other.

Using (2.3) we now find for (5.1):

$$E = -\frac{\rho R}{2}\int_0^{2\pi}\{\Phi_+(\varphi)-\Phi_-(\varphi)\}\frac{\partial\Phi}{\partial n}(\varphi)\,f(\varphi)\,d\varphi\,, \tag{5.4}$$

where $\partial\Phi/\partial n(\varphi)$ is the derivative with respect to the normal $\boldsymbol{n}$ of the cycloid (Fig. 5.1 and formula (3.1)) in a point φ at the cycloid. The potential values $\Phi_+(\varphi)$ and $\Phi_-(\varphi)$ are defined in section 4. Their difference satisfies the relation (4.3), replacing φ_0 by φ. In order to give an expression for $\partial\Phi/\partial n(\varphi)$ we make use of (5.2). It follows, that for a point (x, y) holds:

$$\frac{\partial\Phi}{\partial x}, \frac{\partial\Phi}{\partial y} = \frac{1}{4\pi\mu}\int_0^{2\pi}\gamma(\theta)\left\{\frac{\sinh\left(\frac{y-\eta}{\mu R}\right), -\sin\left(\frac{x-\xi}{\mu R}\right)}{\cosh\left(\frac{y-\eta}{\mu R}\right)-\cos\left(\frac{x-\xi}{\mu R}\right)}\right\}f(\theta)\,d\theta\,. \tag{5.5}$$

With the aid of (3.1) we obtain for $\partial\Phi/\partial n(\varphi)$ the following Cauchy-principle value integral:

$$\frac{\partial\Phi}{\partial n}(\varphi) = -\frac{1}{4\pi\mu}\oint_{l_\varphi}\gamma(\theta)\left\{\frac{\sin\varphi\,\sinh\left(\frac{y-\eta}{\mu R}\right)-(\mu+\cos\varphi)\sin\left(\frac{x-\xi}{\mu R}\right)}{\cosh\left(\frac{y-\eta}{\mu R}\right)-\cos\left(\frac{x-\xi}{\mu R}\right)}\right\}\frac{f(\theta)}{f(\varphi)}\,d\theta\,, \tag{5.6}$$

where the interval of integration l_φ is defined as follows:

$$\text{if } 0\leqq\varphi\leqq d \quad \text{then } l_\varphi \overset{\text{def.}}{=} \{\theta\,|\,-d\leqq\theta\leqq 2\pi-d\}\,,$$

$$\text{if } d<\varphi<2\pi-d \quad \text{then } l_\varphi \overset{\text{def.}}{=} \{\theta\,|\,0\leqq\theta\leqq 2\pi\}\,,$$

$$\text{if } 2\pi-d\leqq\varphi\leqq 2\pi \quad \text{then } l_\varphi \overset{\text{def.}}{=} \{\theta\,|\,d\leqq\theta\leqq 2\pi+d\}\,.$$

By d is meant a small positive value. This shift of the interval of integration in the neighbourhood of $\varphi=0$ and $\varphi=2\pi$ is introduced in order to obtain a principal value integral for $\varphi=0$

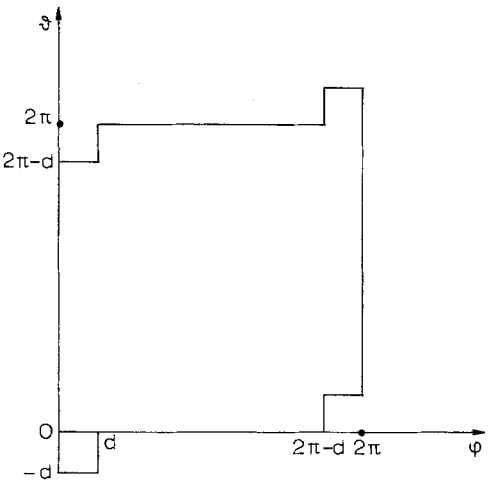

Figure 5.2. Interval of integration as a function of φ.

and $\varphi=2\pi$. Because of the periodicity of the integrand this is allowed. The domain of the integrand is drawn in Fig. 5.2.

We express $\gamma(\theta)$ in $\dot{g}(\theta)$ according to (2.9). Substituting (5.6) into (5.4) thereafter and making use of (4.3), we find:

$$E = \int_0^{2\pi} \left\{ \oint_{l_\varphi} g(\varphi)\, \dot{g}(\theta)\, L(\varphi, \theta)\, d\theta \right\} d\varphi \,, \tag{5.7}$$

where

$$L(\varphi, \theta) = -\frac{\rho}{8\pi\mu} \left\{ \frac{\sin\varphi \sinh\left(\frac{y-\eta}{\mu R}\right) - (\mu + \cos\varphi) \sin\left(\frac{x-\xi}{\mu R}\right)}{\cosh\left(\frac{y-\eta}{\mu R}\right) - \cos\left(\frac{x-\xi}{\mu R}\right)} \right\},$$

with

$$x + iy = R(\mu\varphi + \sin\varphi + i\cos\varphi)$$

and

$$\xi + i\eta = R(\mu\theta + \sin\theta + i\cos\theta)\,.$$

6. The Variational Problem

Before discussing the variational problem, we introduce dimensionless quantities. We agree, that barred symbols are dimensionless:

$$\begin{aligned} &x = \bar{x}R,\ y = \bar{y}R,\ \xi = \bar{\xi}R,\ \eta = \bar{\eta}R,\ s = \bar{s}R;\ \varphi = \bar{\varphi},\ \theta = \bar{\theta}, \\ &K_x = \bar{K}_x \rho\omega^2 R^3\,, \\ &E = \bar{E}\rho\omega^2 R^4\,, \\ &\Gamma(\varphi, s) = \bar{\Gamma}(\bar{\varphi}, \bar{s})\omega R\,, \\ &g(\varphi) = \bar{g}(\bar{\varphi})\omega R^2\,, \\ &L(\varphi, \theta) = \bar{L}(\bar{\varphi}, \bar{\theta})\rho\,. \end{aligned} \tag{6.1}$$

From this moment we use only dimensionless quantities and we omit the bars above the symbols in the following.

Hence, instead of (3.6) and (5.7) there holds for the thrust and the kinetic energy:

$$K_x = \frac{1}{2\pi} \int_0^{2\pi} g(\varphi) \sin\varphi\, d\varphi\,, \tag{6.2}$$

$$E = \int_0^{2\pi} \left\{ \oint_{l_\varphi} g(\varphi)\dot{g}(\theta) L(\varphi, \theta) d\theta \right\} d\varphi\,, \tag{6.3}$$

where

$$L(\varphi, \theta) = -\frac{1}{8\pi\mu} \left\{ \frac{\sin\varphi \sinh\left(\frac{y-\eta}{\mu}\right) - (\mu + \cos\varphi) \sin\left(\frac{x-\xi}{\mu}\right)}{\cosh\left(\frac{y-\eta}{\mu}\right) - \cos\left(\frac{x-\xi}{\mu}\right)} \right\}, \tag{6.4}$$

with

$$x + iy = \mu\varphi + \sin\varphi + i\cos\varphi$$

and

$$\xi + i\eta = \mu\theta + \sin\theta + i\cos\theta\,.$$

It is our aim to choose $g(\varphi)$ in such a way, that E in (6.3) is as small as possible with the subsidiary condition, that K_x in (6.2) has a prescribed value. Because the following symmetry property for $L(\varphi, \theta)$ is valid:

$$L(\varphi, \theta) = -L(2\pi - \varphi, 2\pi - \theta)\,, \tag{6.5}$$

there holds in analogy with [6], section 4, that $g(\varphi)$ has to be an odd function $g_0(\varphi)$ of φ, apart from an arbitrary constant c:

$$g(\varphi) = g_0(\varphi) + c\,. \tag{6.6}$$

In the following we assume the value zero for c. In the case of a wing of finite span, which can be represented by a lifting line, this value for c follows from the considerations in [7], section 5. There it is proved, that the bound vorticities of a wing, represented by a lifting line, in two consecutive positions on a straight line, parallel to the direction of motion, are opposite to each other. It must be stressed, however, that within the scope of our two-dimensional theory this choice for c is arbitrary. Because

$$c = 0 = -\frac{1}{2\pi}\int_0^{2\pi} g_0(\varphi)\left(1 + \frac{\cos\varphi}{\mu}\right)d\varphi \tag{6.7}$$

we see at once, that the mean force K_y in (3.7) becomes zero automatically.

As is expressed by (6.6) and (6.7), $g(\varphi)$ is an odd function. We represent $g(\varphi)$ by a Fourier sine series. We can then solve the variational problem with the use of Ritz's method. Suppose, $g^{(N)}(\varphi)$ is an approximate solution:

$$g^{(N)}(\varphi) = \sum_{j=1}^{N} a_j^{(N)} \sin j\varphi \approx g(\varphi)\,. \tag{6.8}$$

The coefficients in these series generally depend on N, because they are not determined by orthogonality relations. The first coefficient, however, follows directly from condition (6.2):

$$a_1^{(N)} = 2K_x\,. \tag{6.9}$$

By minimizing the energy E, we find the remaining coefficients. Substitution of (6.8) into (6.3) gives

$$E \approx E^{(N)} \overset{\text{def.}}{=} \sum_{p,q=1}^{N} q a_p^{(N)} a_q^{(N)} \int_0^{2\pi}\left\{\oint_{l_\varphi} \sin p\varphi \cos q\theta\, L(\varphi,\theta)\,d\theta\right\} d\varphi =$$

$$\overset{\text{def.}}{=} \sum_{p,q=1}^{N} q a_p^{(N)} a_q^{(N)} L^{p,q}\,. \tag{6.10}$$

For a minimum of $E^{(N)}$ it is necessary, that

$$\frac{\partial E^{(N)}}{\partial a_j^{(N)}} = 0 \qquad (j = 2, \ldots, N)\,.$$

Hence, we obtain the following system of linear equations for the coefficients $a_j^{(N)}$ $(j = 2, \ldots, N)$:

$$\sum_{p=2}^{N} a_p^{(N)}(pL^{n,p} + nL^{p,n}) = -a_1^{(N)}(L^{n,1} + nL^{1,n})\,, \qquad (n = 2, \ldots, N)\,. \tag{6.11}$$

It follows from (6.9) and (6.11), that all coefficients $a_j^{(N)}$ depend on K_x linearly. Thus the optimal vorticity function $g(\varphi)$ is proportional to K_x. This fact will be used later on.

It can be proved easily [9] that $L^{n,p}$ and $L^{p,n}$ satisfy the relation

$$pL^{n,p} = nL^{p,n}\,. \tag{6.12}$$

7. Another Description of the Wake of the Optimum Propeller

In section 6 we have set up a variational problem for the vorticity function $g(\varphi)$. However, there is another way of obtaining knowledge about $g(\varphi)$. In [1] Betz has developed a theory about the behaviour of the free vorticity behind an optimal screw propeller. It is shown in [7], that this theory can be adapted to a class of nonstationary propellers, to which belongs our cycloidal propeller.

We start with the prescribed mean thrust K_x. Using dimensionless quantities, there holds according to (3.5):

$$K_x = \frac{1}{2\pi}\int_0^{2\pi}\left\{\int_a^{a+l} G(\psi, s)\sin\varphi\frac{f(\psi)}{f(\varphi)}\,ds\right\}d\psi\,.$$

When $G(\psi, s)$ is the optimal bound vorticity distribution, we will consider (see [7]) such variations of $G(\psi, s)$, that

$$\Delta K_x = \frac{1}{2\pi}\int_0^{2\pi}\left\{\int_a^{a+l}\Delta G(\psi, s)\sin\varphi\frac{f(\psi)}{f(\varphi)}\,ds\right\}d\psi = 0\,. \tag{7.1}$$

Introducing the vorticity function $g(\varphi)$, we may also write, in accordance with (3.6):

$$\Delta K_x = \frac{1}{2\pi}\int_0^{2\pi}\Delta g(\varphi)\sin\varphi\,d\varphi = 0\,. \tag{7.2}$$

Using (2.4) we find for the linear part of the variation ΔE of the kinetic energy E far behind the segment AB from formula (4.3) of [7]:

$$\Delta E = -\int_0^{2\pi}\left\{\int_a^{a+l}\Delta G(\psi, s) f(\psi) w_n(\varphi)\,ds\right\}d\psi\,, \tag{7.3}$$

where $w_n(\varphi)$ denotes the normal velocity at the point φ at the cycloid, supposing the segment AB is at $x = +\infty$. The vorticity function $G(\psi, s)$ has a positive value, if the corresponding flow is counterclockwise and $w_n(\varphi)$ is positive in the direction of the normal $\boldsymbol{n}$ (Fig. 2.2). We have reduced (7.1) to (7.2). In an analogous way we may reduce (7.3) to

$$\Delta E = -\int_0^{2\pi}\Delta g(\varphi) w_n(\varphi) f(\varphi)\,d\varphi\,. \tag{7.4}$$

This expression for ΔE, based on (4.3) of [7], is obtained by purely mechanical reasoning. It is also possible to check (7.4) in an analytical way [9].

When $g(\varphi)$ is the optimal vorticity function, the functional ΔE in (7.4) has to be zero for all variations $\Delta g(\varphi)$, which satisfy (7.2). Besides the functionals ΔE and ΔK_x, defined on the linear space of continuous functions $\Delta g(\varphi)$, are linear.Hence, according to [3],

$$\Delta E - u\Delta K_x = 0$$

for an arbitrary variation $\Delta g(\varphi)$, with u some unknown constant. This yields:

$$w_n(\varphi) = -u\frac{\sin\varphi}{f(\varphi)}\,. \tag{7.5}$$

In order to connect this result with the more general results of [7], we consider the, in the x-direction two-sided infinitely long, cycloidal surface passed through by the blade after an infinitely long time. When we place this surface in a homogeneous flow with a velocity u parallel to the x-axis, we find that the normal component of the velocity equals (7.5).

This means that the vorticity needed to make this surface a stream surface equals the vorticity $\gamma(\varphi)$ shed by the optimal cycloidal propeller.

From (6.6) it follows, that $g(\varphi)$ has to be an odd function, apart from a constant. Also we can prove this by starting from the above-mentioned condition. In [7] it is shown by symmetry considerations, that $\gamma(\varphi)$ is an even function of φ. Then application of (2.9) learns, that $\dot{g}(\varphi)$ is an even function. Consequently $g(\varphi)$ is an odd function, when the value zero is chosen for the additive constant.

Now it is possible to find $g(\varphi)$ from a mixed boundary-value problem. We consider the "frozen" cycloid in a homogeneous flow with velocity $u = 1$ in the positive x-direction. Suppose this "frozen" cycloid can be represented by the bound vorticity distribution $\gamma_1(\varphi)$. Then $\gamma_1(\varphi)$ is the free vorticity behind the optimum propeller for the case $u = 1$. Suppose, next, that $g_1(\varphi)$ denotes the vorticity function $g(\varphi)$, which belongs to the free vorticity $\gamma_1(\varphi)$ by (2.9). Then there must hold, according to (4.3), for the jump in the velocity potential Φ_1 across the "frozen" cycloid:

$$\Phi_{1+}(\varphi)-\Phi_{1-}(\varphi)=g_1(\varphi)\,. \tag{7.6}$$

In connection with the periodicity and symmetry we confine ourselves to half a period of the cycloid. We see, using (2.1) and (6.1), that we have to solve the following boundary-value problems for two unbounded regions:

$$\frac{\partial^2\Phi_{1\pm}(x,y)}{\partial x^2}+\frac{\partial^2\Phi_{1\pm}(x,y)}{\partial y^2}=0\,, \tag{7.7}$$

with

$$x=0,\ y\gtrless 1: \qquad \Phi_{1\pm}(x,y)=0\,,$$
$$x=\pi\mu,\ y\gtrless -1: \qquad \Phi_{1\pm}(x,y)=\pi\mu\,,$$
$$x=\mu\varphi+\sin\varphi,\ y=\cos\varphi,\ 0\leqq\varphi\leqq\pi: \frac{\partial\Phi_{1\pm}(\varphi)}{\partial n}=0\,.$$

Having solved these problems, we can find the limit values $\Phi_{1+}(\varphi)$ and $\Phi_{1-}(\varphi)$ in a point φ at the cycloid. Then we obtain $g_1(\varphi)$ from (7.6). By reasons of linearity it follows from (7.6) and (7.7), that

$$g(\varphi)=ug_1(\varphi)\,, \tag{7.8}$$

while we deduce from (6.2) for u, that

$$u=2\pi K_x\left\{\int_0^{2\pi} g_1(\theta)\sin\theta\,d\theta\right\}^{-1}\,. \tag{7.9}$$

Another possibility of getting $\Phi_{1+}(\varphi)$ and $\Phi_{1-}(\varphi)$ is by solving the potential problem by means of an electrolytic tank. A description of such a tank is given in [4]. We can simulate the flow along the rigid cycloid, if we place flat conductors along the lines $x=0$ and $x=\pi\mu$, with a

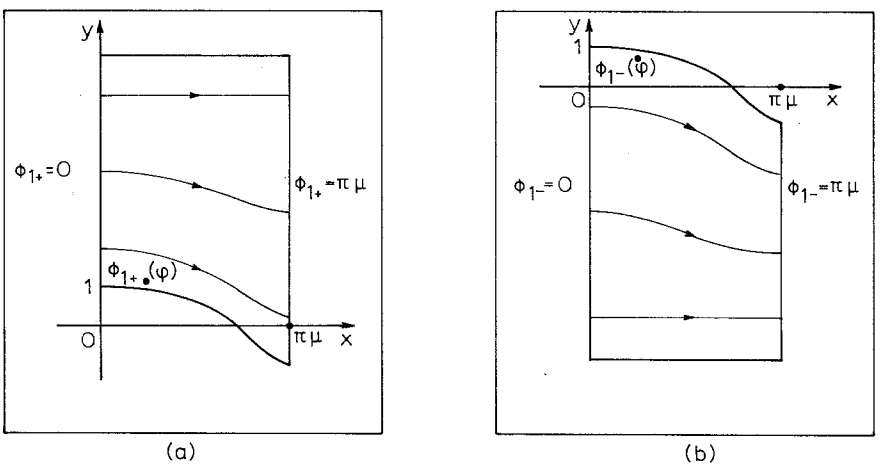

Figure 7.1. Electrolytic tank configurations.

potential difference $\pi\mu$, and an insulator along the cycloid (Fig. 7.1). Because of the unboundedness of the regions we have to place at a "sufficiently large" distance from the cycloid an insulator parallel to the x-axis. Measuring the potential values $\Phi_{1+}(\varphi)$ (Fig. 7.1a) and $\Phi_{1-}(\varphi)$ (Fig. 7.1b) along the cycloidal insulators at corresponding points, we can obtain the function $g_1(\varphi)$. We remark, however, that it is not necessary to measure both $\Phi_{1+}(\varphi)$-values and $\Phi_{1-}(\varphi)$-values. For, it can be proved easily, that the following relation holds:

$$\tfrac{1}{2}\{\Phi_{1+}(\varphi)+\Phi_{1-}(\varphi)\}=x(\varphi)\,.$$

Results of such a measurement are given in section 10 where they are compared with numerical calculations.

8 The Normal Velocity at the Segment AB

In order to calculate the angle of incidence of the profile, we need the normal velocity in each point of the segment AB, induced by the bound and free vorticity.

In the complex plane the point $z=x+iy$ will correspond to the point (φ, s) of AB (Fig. 8.1). ψ denotes, as in the foregoing, the angular coordinate of the reference point T. The induced

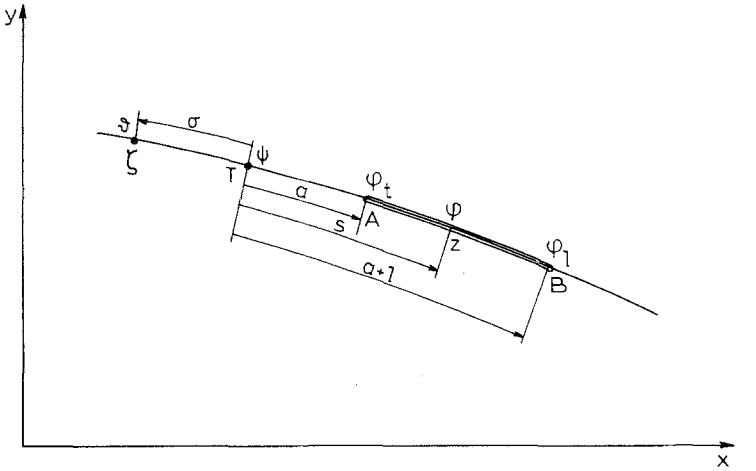

Figure 8.1. The segment AB in the complex $(x+iy)$-plane.

velocity $\boldsymbol{v}$ with components v_x and v_y in the point z as a result of a concentrated vortex Γ at $\zeta=\xi+i\eta$ is

$$v_x-iv_y=\frac{\Gamma}{2\pi i(z-\zeta)},$$

where Γ is assumed again to be positive, if the corresponding flow is counterclockwise. When the point ζ lies at the cycloid, we find $\zeta=\zeta(\theta)$ from (5.3).

We denote the angular variables of the trailing edge and leading edge of segment AB with respectively φ_t and φ_l. Using (3.3) and (2.3) and integrating, we find for the velocity $\boldsymbol{v}_1(\psi, \varphi)$, with components v_{1x} and v_{1y}, induced by the free vorticity behind AB, at the point (φ, s) of AB:

$$v_{1x}-iv_{1y}=\frac{1}{2\pi i}\int_{-\infty}^{\varphi_t}\frac{\gamma(\theta)f(\theta)}{\mu(\varphi-\theta)+\sin\varphi-\sin\theta+i\,(\cos\varphi-\cos\theta)}\,d\theta. \tag{8.1}$$

Hence, using (2.9) and (3.1), the component $v_{1n}(\psi,\varphi)$ of the velocity $\boldsymbol{v}_1(\psi,\varphi)$, normal to the cycloid, becomes

$$v_{1n}(\psi,\varphi)=-\frac{1}{2\pi f(\varphi)}\int_{-\infty}^{\varphi_t}\dot{g}(\theta)M(\varphi,\theta)d\theta\,, \tag{8.2}$$

where

$$M(\varphi,\theta)=\frac{-\mu\{(\mu+\cos\varphi)(\theta-\varphi)+(\sin\theta-\sin\varphi)\}+\sin(\theta-\varphi)}{\mu^2(\theta-\varphi)^2+2\mu(\theta-\varphi)(\sin\theta-\sin\varphi)+2-2\cos(\theta-\varphi)}. \tag{8.3}$$

In the same way we obtain the normal component $v_{2n}(\psi,\varphi)$ of $\boldsymbol{v}_2(\psi,\varphi)$, the velocity caused by the free vorticity along AB:

$$v_{2n}(\psi,\varphi)=\frac{1}{2\pi f(\varphi)}\int_{\varphi_t}^{\varphi_l}\gamma(\theta,\sigma)f(\theta)M(\varphi,\theta)d\theta\,. \tag{8.4}$$

By $\sigma=\sigma(\psi,\theta)$ we mean the distance from T to a variable point at the cycloid, measured along the cycloid (Fig. 8.1). This distance is positive in the translation direction of segment AB.

Using (3.3) we find:

$$\sigma = \int_{\psi}^{\theta} f(\chi)\,d\chi\,. \tag{8.5}$$

For the normal component $v_{3n}(\psi, \varphi)$ of $v_3(\psi, \varphi)$, the velocity, induced by the bound vorticity of AB, we find the following Cauchy-principal value integral:

$$v_{3n}(\psi, \varphi) = \frac{1}{2\pi f(\varphi)} \oint_{\varphi_t}^{\varphi_l} G(\psi, \sigma) f(\theta) M(\varphi, \theta)\,d\theta\,. \tag{8.6}$$

9. The Angle of Incidence of the Rigid and Flat Profile

We now consider the optimal motion of the profile. The variations of the angle of incidence as a function of time have to be chosen so, that the desired free vorticity $\gamma(\varphi)$ will be shed off. This free vorticity follows directly by (2.9) from the optimal function $g(\varphi)$, the solution of the variational problem of section 6. Nothing yet is known about the distribution of the bound vorticity

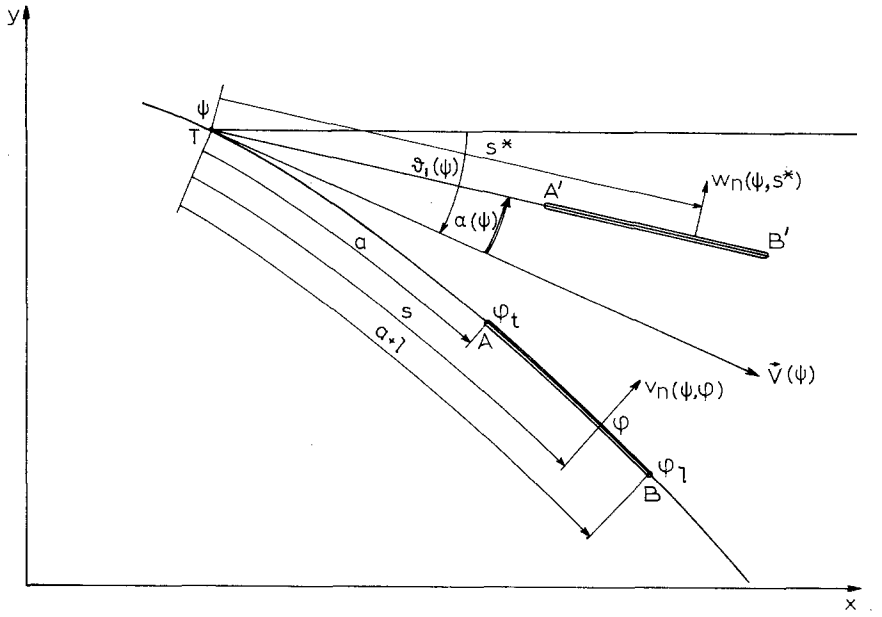

Figure 9.1. The angle of incidence of the rigid and flat profile.

$G(\psi, s)$ or $\Gamma(\varphi, s)$ along the segment AB. Therefore we suppose, that we have the freedom to choose the shape of the profile. We take a rigid and flat profile, oscillating around the turning point T (Fig. 9.1).

We assume [2] the following expression for $\Gamma(\varphi, s)$:

$$\Gamma(\varphi, s) = e_{-2}(\varphi)(a+l-s)^{-\frac{1}{2}} + e_{-1}(\varphi)(s-a)^{\frac{1}{2}} + \sum_{m=0}^{M} e_m(\varphi)(s-a)^m\,. \tag{9.1}$$

The $e_m(\varphi)$ will be bounded periodic functions with period 2π ($m = -2, -1, 0, 1, \ldots M$). The Kutta-condition reads

$$\Gamma(\varphi, a) = l^{-\frac{1}{2}} e_{-2}(\varphi) + e_0(\varphi) = 0\,. \tag{9.2}$$

After substituting (9.1) into (2.8) and integrating, we find the following expression for $g(\varphi)$:

$$g(\varphi) = 2l^{\frac{1}{2}} e_{-2}(\varphi) + \tfrac{2}{3} l^{\frac{3}{2}} e_{-1}(\varphi) + \sum_{m=0}^{M} \frac{l^{m+1}}{m+1} e_m(\varphi)\,. \tag{9.3}$$

The normal velocities $v_{2n}(\psi, \varphi)$ and $v_{3n}(\psi, \varphi)$, given by respectively (8.4) and (8.6), can now be expressed into the coefficients $e_m(\varphi)$ of (9.1) by using (2.6) and (3.2).

We next investigate the normal velocity $w_n(\psi, s^*)$ at a point of the profile A'B' (Fig. 9.1), caused by the angle of incidence and the oscillatory motion of the profile. By s^* we mean the distance from T to a point at the profile (Figs. 2.1 and 9.1). The angle of incidence $\alpha(\psi)$ of the profile will be the angle between the profile and the tangent to the cycloid in T in case of an optimum propeller, when the mean thrust has some value K_x. We agree, $\alpha(\psi)$ is positive in counterclock direction. The contribution of the velocity vector $V(\psi)$ to the normal component $w_n(\psi, s^*)$ is independent of the position s^* at the profile:

$$w_{1n}(\psi, s^*) = \alpha(\psi) f(\psi) . \tag{9.4}$$

Because our theory is linear, we suppose, $|\alpha(\psi)|$ is sufficiently small. Also the oscillatory motion of the profile around T yields a contribution to the normal velocity. Using (2.2) we find:

$$w_{2n}(\psi, s^*) = -s^* \frac{d}{dt} \{\alpha(\psi) + \theta_1(\psi)\} = -s^* \left(\frac{d\alpha}{d\psi} + \frac{d\theta_1}{d\psi} \right), \tag{9.5}$$

where $\theta_1(\psi)$ represents the angle between the tangent to the cycloid in T and the fixed x-direction, again positive in counterclock direction. In accordance with (2.1) there holds for $\theta_1(\psi)$:

$$\theta_1(\psi) = -\operatorname{arctg} \frac{\sin \psi}{\mu + \cos \psi} .$$

Making use of (2.3) we find:

$$\frac{d\theta_1(\psi)}{d\psi} = -\frac{\mu \cos \psi + 1}{\{f(\psi)\}^2} . \tag{9.6}$$

In the foregoing we supposed $|\alpha(\psi)|$ to be small. Also the angle between the tangents to the cycloid in A and B will be small, because we consider a profile, the length of which is small with respect to the smallest radius of curvature of the cycloid. Therefore we use a linearization procedure (section 2) and compare the normal velocity, induced by the vorticity at the cycloid, with the velocity $w_n(\psi, s^*)$, caused by the angle of incidence and the oscillatory motion. The following equation for the normal velocities will hold:

$$-\sum_{i=1}^{2} w_{in}(\psi, s^*) = -w_n(\psi, s^*) = v_n(\psi, \varphi) = \sum_{i=1}^{3} v_{in}(\psi, \varphi), \text{ if } s^* = s , \tag{9.7}$$

where $s = s(\psi, \varphi)$ according to (3.3).

From this equation we are able to evaluate the angle $\alpha(\psi)$.

In order to obtain $\alpha(\psi)$ for different values of K_x it is not necessary to perform all calculations anew for each K_x. For, we can make use of the following relation, which is easily proved [9]:

$$\alpha(\psi) = \alpha_0(\psi) + K_x \{\alpha_1(\psi) - \alpha_0(\psi)\} , \tag{9.8}$$

where we mean by $\alpha_1(\psi)$ and $\alpha_0(\psi)$ the "angles of incidence", which belong to respectively $K_x = 1$ and $K_x = 0$. We notice, that $K_x = 0$ implies $g(\varphi) \equiv 0$, as is obvious from the remark at the end of section 6.

We see, that the geometrical angle of incidence consists of two parts, viz. a part, which delivers a mean thrust zero and an effective part, which is proportional to the mean thrust.

10. Results

In this section we give results for the optimal vorticity function $g(\varphi)$ and the efficiency, which belongs to it. This efficiency is compared with the efficiency of the two-dimensional actuator disc, which has the highest possible efficiency, for a given velocity of advance, working area and mean thrust [8]. Angles of incidence $\alpha(\psi)$ of the optimum propeller have been calculated for two different chord lengths l in order to investigate the influence of l upon $\alpha(\psi)$. Moreover

these results for $\alpha(\psi)$ are compared with the results, following from the theory of [6], which treats the blade as a lifting line.

For the constant μ in (2.1) the value 1.6 is chosen. This yields a cycloidal orbit for the segment AB, which is drawn in Fig. 10.1. We deduce from (2.1) for the smallest radius of curvature ρ_s, that

$$\rho_s = (\mu - 1)^2 .$$

Hence, if $\mu = 1.6$, then the length l of segment AB has to be theoretically much smaller than 0.36. We have performed calculations for $l = 0.1$ and $l = 0.15$ (Fig. 10.1).

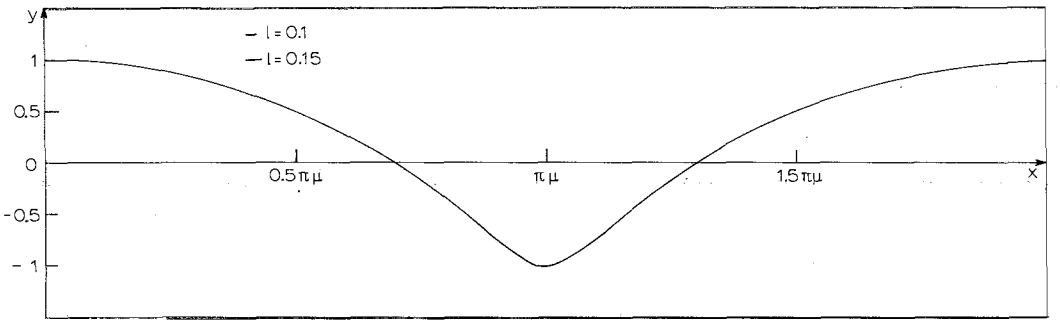

Figure 10.1. The cycloidal orbit of segment AB ($\mu = 1.6$).

The optimal vorticity function $g(\varphi)$ can be calculated from (6.9) and (6.11). If we take $K_x = 1$ in (6.9), then the first coefficient has the value 2. For successive values of N the coefficients $a_j^{(N)}$, together with the corresponding value $E^{(N)}$ for the kinetic energy, defined by (6.10), are given in table 10.1. With increasing N the $a_j^{(N)}$ remain almost constant for a fixed j, while with increasing j the $a_j^{(N)}$ approach to zero rapidly. It is obvious from (6.10) and (6.11), that with increasing N the value for $E^{(N)}$ decreases. It turns out, that $E^{(4)}$ and $E^{(5)}$ are equal within the used accuracy. Hence $E^{(5)}$ is a good approximation for the minimal kinetic energy E, and $g(\varphi)$ is approximated sufficiently accurate by a sine series of 4 or 5 terms.

TABLE 10.1

The coefficients $a_j^{(N)}$ and the kinetic energy $E^{(N)}$ ($K_x = 1$).

$a_j^{(N)}$	$j=1$	$j=2$	$j=3$	$j=4$	$j=5$	$E^{(N)}$
$N=1$	2					3.75518
$N=2$	2	0.07744				3.74529
$N=3$	2	0.07716	−0.01118			3.74499
$N=4$	2	0.07715	−0.01117	0.00118		3.74498
$N=5$	2	0.07715	−0.01117	0.00118	−0.00007	3.74498

In Fig. 10.2 $g(\varphi)$ is compared with the result, obtained by electrolytic measurements (section 7). We remark a small difference between the both graphs. Probably this is due to systematic errors of the electrolytic tank.

It is now easy to express the efficiency η_0 of our optimum cycloidal propeller into the mean thrust K_x. According to (6.3), Table 10.1 and the fact, that the optimal function $g(\varphi)$ is proportional to K_x, as is derived in section 6, we find for the kinetic energy E, left behind in the wake per period, that

$$E = 3.74\,(K_x)^2, \text{ if } \mu = 1.6 .$$

From section 3 follows for the useful work E_u of the thrust per period:

$$E_u = 2\pi\mu K_x .$$

Therefore

$$\eta_0 = \frac{E_u}{E_u+E} = (1+0.373\,K_x)^{-1}, \text{ if } \mu = 1.6\,. \tag{10.1}$$

In [8] it is proved, that the highest possible efficiency η_i of a propeller with a certain working area, velocity of advance and mean value of thrust, is given by the efficiency of the actuator disc with the same three characteristic quantities.

It is easy to show, that in the two-dimensional theory there holds for an actuator disc, making use of the dimensionless quantities of (2.1) and (6.1),

$$\eta_i = \left(1 + \frac{K_x}{4\mu^2}\right)^{-1}$$

Hence, we obtain

$$\eta_i = (1-0.098K_x)^{-1}, \text{ if } \mu = 1.6\,. \tag{10.2}$$

We stress, that (10.1) denotes the efficiency of the optimum cycloidal propeller with one blade.

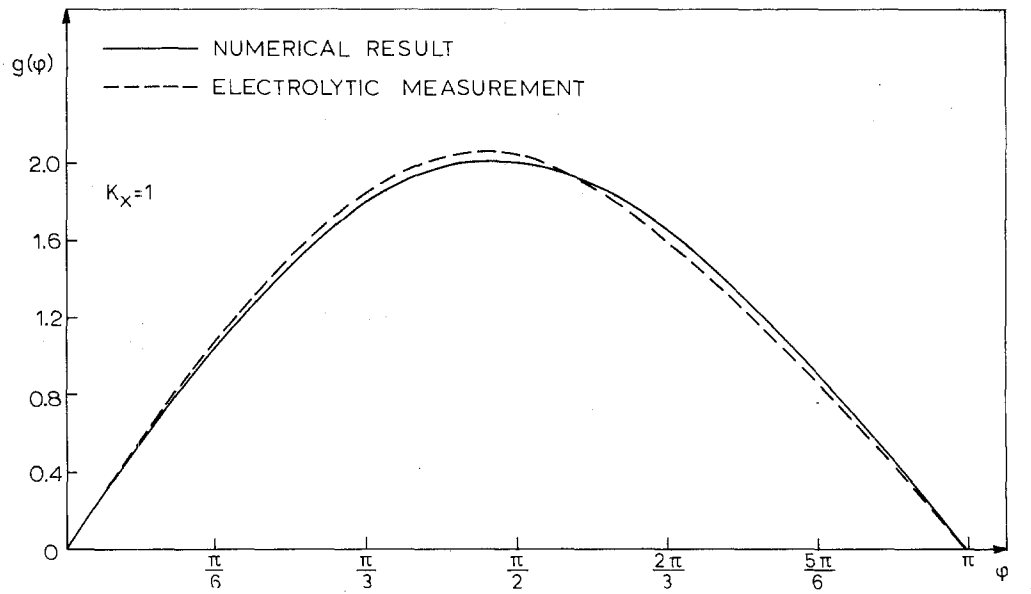

Figure 10.2. The vorticity function $g(\varphi)$.

From [6], section 6, it follows, that the actuator disc can be "realised" by a cycloidal propeller with an infinite number of blades. Hence, we expect, that with the increase of the number of blades the efficiency η_0 of the optimum propeller will increase and approach η_i, given by (10.2). It may be remarked, that even in the case of a one-bladed vertical axis propeller, which delivers the same mean thrust, has the same velocity of advance and the same working area [8], the efficiency can be made equal to η_i. However, then the blade has to follow not a cycloidal, but another, rather complicated, although perhaps technical possible, path.

The quality coefficient q which we define as the ratio of the coefficients of K_x in (10.2) and (10.1) is

$$q = \frac{0.098}{0.373} = 0.263\,. \tag{10.3}$$

Because the actuator disc has the highest possible efficiency, we have $0 \leqq q \leqq 1$. It turns out that this two-dimensional, one-bladed propeller, even in optimum condition, is a propulsion device with a low quality coefficient.

Of course its efficiency can be high when K_x is small, however when K_x increases, the efficiency decreases much faster than the efficiency of the actuator disc. From this it follows that also a fish has, from the point of view of potential flow, a low quality propulsion.

We now mention the results of the calculations of the angle of incidence as a function of time or of the position of the profile along the cycloid.

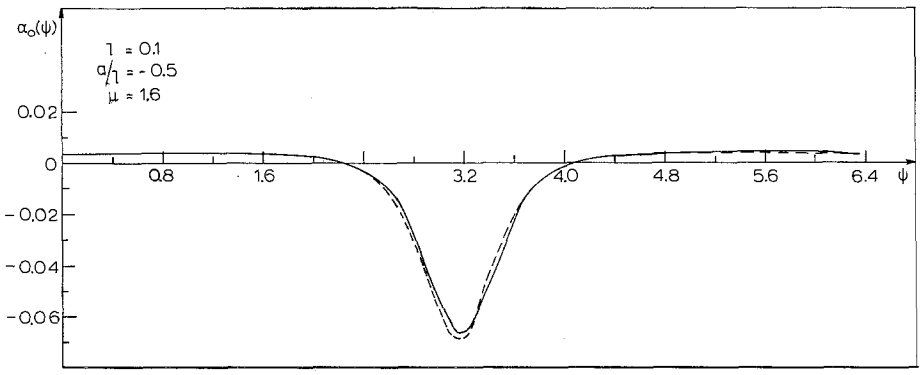

Figure 10.3. The angle of incidence for $l=0.1$ and $K_x=0$ (present theory full line, theory of [6] dashed line).

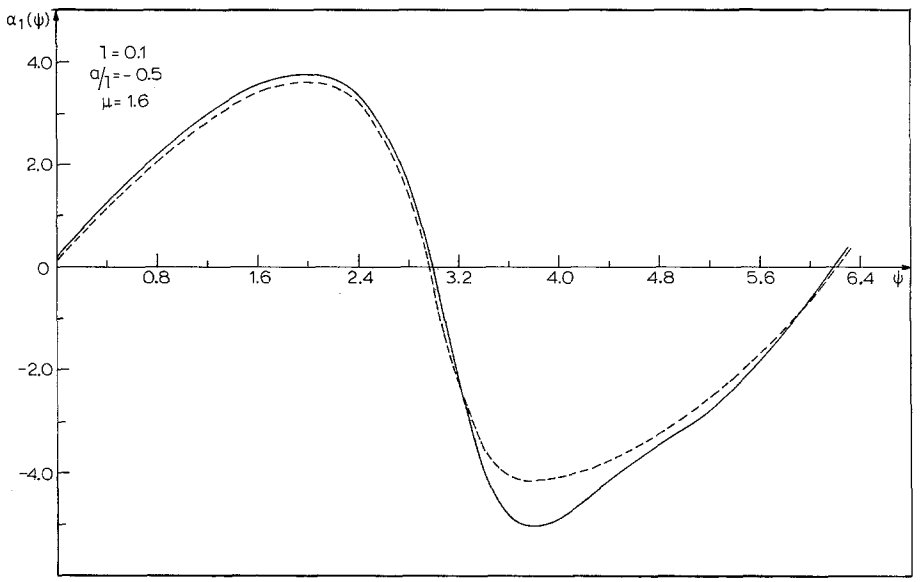

Figure 10.4. The angle of incidence for $l=0.1$ and $K_x=1$ (present theory full line, theory of [6] dashed line).

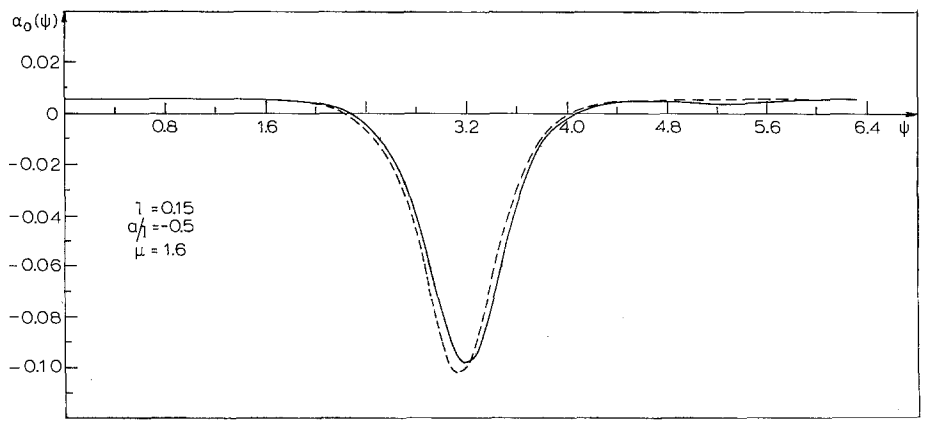

Figure 10.5. The angle of incidence for $l=0.15$ and $K_x=0$ (present theory full line, theory of [6] dashed line).

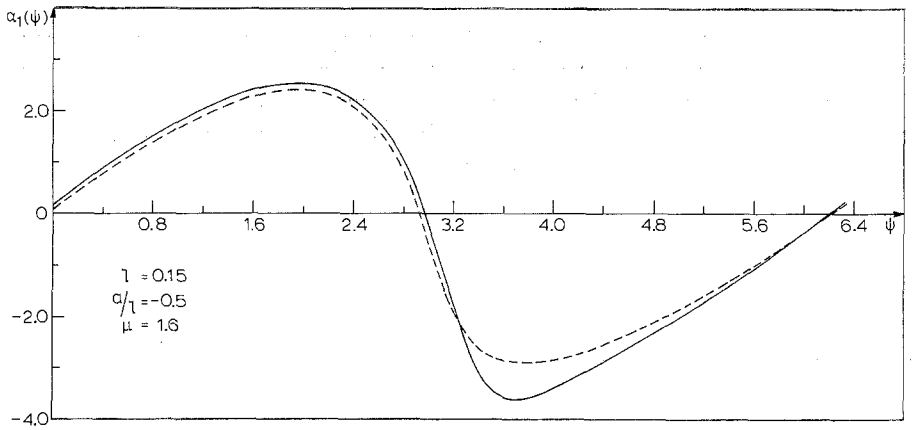

Figure 10.6. The angle of incidence for $l=0.15$ and $K_x=1$ (present theory full line, theory of [6] dashed line).

For the length l of segment AB we take first the value 0.1, while the reference point T (Fig. 9.1) is chosen in the middle of the profile, hence $a=-\frac{1}{2}l$. In Figs. 10.3 and 10.4 the full line denotes respectively the angle of incidence $\alpha_0(\psi)$ and $\alpha_1(\psi)$ (9.8), calculated with the theory of this paper. The results obtained from the lifting line theory of [6], are represented by the dashed lines. It is seen that, although there are differences, certainly a good conformity exists.

In the case that $l=0.15$ the results are given in the Figs. 10.5 and 10.6. We remark that with increasing l the absolute values of the angle of incidence decrease almost proportional to l^{-1}. In fact the pressure distribution at a blade with a larger chord length, has to be smaller in order to deliver the same total thrust.

Acknowledgements

The numerical calculations were performed for the most part on the Stantec Zebra computer and the TR4 computer of the "Computing Centre" of the Groningen University. The authors are indebted to the staff of this centre for their assistance, particularly to Mr. D. Velvis, who wrote the necessary Algol programs.

Thanks are due to the "Netherlands Ship Model Basin" at Wageningen, where a part of the calculations for the function $g(\varphi)$ has been carried out on the X1 computer.

Also the authors are indebted to Dr. J. L. Verster of the "Technical Physical Laboratory" of the Groningen University, under whose supervision Mr. F. P. C. Visser measured, by means of an electrolytic tank, the function $g(\varphi)$.

REFERENCES

[1] Betz, A.: *Schraubenpropeller mit geringsten Energieverlust*; Nachrichten von der Königlichen Gesellschaft der Wissenschaften zu Göttingen, Math.-phys. Klasse, Heft 2, Berlin, 1919.

[2] Bisplinghoff, R. L., Ashley, A. and Halfman, R. L.: *Aeroelasticity*; Addison-Wesley Publishing Company, Inc., Reading, Massachusetts, 2nd printing, 1957.

[3] Gelfand, I. M. and Fomin, S. V.: *Calculus of Variations*; translated by R. A. Silverman, Prentice-Hall, Inc., Englewood Cliffs, New Yersey, 1963.

[4] Karplus, W. J.: *Analog Simulation. Solution of field problems*; McGraw-Hill Book Company, 1958.

[5] Mueller, H. F.: *Recent Developments in the Design and Application of the Vertical Axis Propeller*; The Society of Naval Architects and Marine Engineers, New York, 1955.

[6] Sparenberg, J. A.: *On the efficiency of a vertical-axis propeller*; Third Symposium Naval Hydrodynamics, high performance ships; *N.S.P.*, Wageningen, 1960.

[7] Sparenberg, J. A.: *On the efficiency of a class of nonstationary ship propellers*; Journal of Ship Research, December, 1967.

[8] Sparenberg, J. A.: *An Upper Bound for the Efficiency of Lightly Loaded Ship Propellers*; Volume 110, Transactions R.I.N.A., No. 1, 1968.

[9] Sparenberg, J. A. and de Graaf, R.: "*On the optimum one-bladed cycloidal ship propeller*"; Report TW-50, Math. Inst., University of Groningen, Holland, 1967.